Int. J. Heat Mass Transfer. Vol. 28, No. 11, pp. 2129–2136, 1985
Printed in Great Britain

0017-9310/85 $3.00 + 0.00

Governing equations for heat and mass transfer in heat-generating porous beds—I. Coolant boiling and transient void propagation*

T. C. CHAWLA,† D. R. PEDERSEN† and W. J. MINKOWYCZ‡

†Reactor Analysis and Safety Division, Argonne National Laboratory, Argonne, IL 60439, U.S.A.
‡Department of Mechanical Engineering, University of Illinois at Chicago, Chicago, IL 60680, U.S.A.

(*Received* 10 *March* 1985 *and in final form* 23 *May* 1985)

Abstract—It has been proposed as a reactor design option to line the bottom of the guard vessel with magnesia (MgO) bricks to retain the core debris following a core-disruptive accident. With conduction as the dominant mode of heat transfer in the debris bed and natural convection in the overlying pool, the debris bed, while fully submerged in sodium coolant, may begin to heat up and lead to coolant boiling. During boiling, to determine transient void distribution, a void propagation equation is derived. The transient aspects of the void distribution are expected to be important for very deep beds and during debris bed quenching. The vapor production source term is obtained from the solution of energy equation for the two-phase coolant, whereas the temperature distribution in the solid phase is calculated from the conduction equation. The heat flux from the fuel particulate to the two-phase coolant is modeled from the solution of steady-state two-phase continuity, momentum and energy equations.

INTRODUCTION

IN A HYPOTHETICAL accident leading to core meltdown in a liquid metal sodium-cooled fast breeder reactor (LMFBR) or a water-cooled thermal reactor, molten core materials upon contact with sodium or water coolant will rapidly quench, freeze and fragment. These fragments or debris may settle on the bottom of the reactor vessel and form a debris bed. If the amount of fuel contained in the debris bed is not enough to form a critical mass then it is heated only by the radioactive decay of fission products and actinides. The debris bed is generally submerged in sodium or water coolant. If the bed is deep enough and the cooling is not adequate in part of the bed, the bed will dry out due to boiloff of the coolant. This will eventually lead to steel and fuel melting. If the reactor vessel is attacked by this molten steel and fuel, then a breach in the reactor vessel will allow molten steel and fuel, and liquid sodium or water to escape into the containment structure and threaten the integrity of the containment building. To guard against this potential for damage to the containment building, it is proposed that MgO brick lining be placed between the reactor vessel and the guard vessel. A sketch of this lining together with the debris bed and overlying sodium pool is shown in Fig. 1. To contain the debris bed within the guard vessel, it is essential to know to what extent the various natural cooling mechanisms available can be relied upon. The purpose of this analysis, to be presented in two parts, is to derive governing equations for determining the degree of penetration by the molten pool formed by the eutectic solution of fuel in MgO. The thickness and heat loading of the debris bed will be varied over a wide range so as to arrive at a 'safe' thickness of brick lining and the required associated degree of external cooling. A general description of the phenomenology leading to debris bed dryout will be discussed here in Part I.

Initially, the fuel debris may consist of fuel and steel particles forming a porous bed submerged in sodium coolant lying on the bottom of the pressure vessel backed by MgO brick (see Fig. 1). During the initial heatup of the bed, because of very high resistance and relatively low porosity ($\sim 45\%$), the dominant mode of heat transfer in the saturated bed is conduction, whereas in the overlying pool (see Fig. 1), natural convection dominates. If the bed height and decay power levels are such that these modes of heat transfer are inadequate, then sodium boiling and dryout may occur.

The objective of the present investigation is to determine dryout heat flux and the void propagation in the bed as a function of time and space. The transient aspects of the void propagation and dryout heat flux are especially important in a deep bed, as the deep bed is likely to dryout earlier in time when the decay heat may still be a strong function of time. Also, in a shallow bed, it is of interest to know how long it takes the bed to dryout and how large the dry zone becomes before it reaches steady state. It is also of interest to know the quench front in the quenching process of the bed by bottom or top flooding. The existing studies, which are numerous (e.g. refs. [1–4]), have concentrated only on quasi-steady determination of dryout heat flux and void distribution. Recently, a study appeared [5] that attempts to perform transient analysis; however, it contains errors in formulation of the governing equations and boundary conditions and consequently its predictions appear to be nonphysical.

* Work performed under the auspices of the U.S. Department of Energy.

NOMENCLATURE

A_S	total surface area of the solid particles in the bed
a_s	surface area of particles per unit volume of bed
B	total bed loading due to solid particulate [kg m^{-2}]
B_F	bed loading due to fuel particulate [kg m^{-2}]
B_s	bed loading due to steel particulate [kg m^{-2}]
C_p	specific heat at constant pressure
C_{PF}	specific heat of fuel at constant pressure
D	particle diameter
D_α	diffusion coefficient defined by equation (21)
F	symbol defined by equation (20a)
g	acceleration due to gravity
h_f	enthalpy of liquid coolant
h_g	enthalpy of sodium vapor
K	thermal conductivity
$K_{2\Phi}$	thermal conductivity of the two-phase mixture
k	permeability
k_{rf}	relative permeability for liquid phase
k_{rg}	relative permeability of vapor phase
$\dot{m}_v$	mass flux of sodium vapor
N	number of solid particles
P	pressure in the debris bed
P_c	capillary pressure
$\dot{Q}$	heat generation rate per unit volume of bed
q	heat flux
q_w	particle heat flux
$\dot{q}$	heat generation rate per unit volume of fuel
s	saturation of debris bed, i.e. fraction of void volume occupied by liquid sodium coolant
T	temperature
t	time
x, y	local coordinates
Y	position of interfaces in debris bed
Y_F	the position void or quench front at the top
V	volume of debris bed
v_f	interstitial velocity of the liquid in debris bed
v_g	interstitial velocity of vapor in the debris bed
V_α	velocity defined by equation (21b).

Greek symbols

α	$1-s$, void fraction in debris bed
Γ	volumetric generation or condensation rate of sodium vapor
ε	void fraction in the debris bed
ε_F	volume fraction of fuel particulate
ε_s	volume fraction of steel particulate
μ	dynamic viscosity
ν	kinematic viscosity
ρ	density
$\Delta\rho$	$\rho_f-\rho_g$
Δh	h_g-h_f
Φ	defined by equation (20b)
Ψ	defined by equation (20a)
Ω	reaction frequency defined by equation (21c)

Subscripts

E, e	equivalent
F	fuel
f	liquid coolant
D	debris bed
g	sodium vapor
L	lower interface
M	MgO lining
Na	sodium coolant
s	stainless steel
S	solid
SE	solid fuel and steel particulate
U	upper interface.

FORMULATION OF MODEL

Experimental studies [6–10] on steady-state boiling in porous media have demonstrated the existence of an isothermal two-phase region, where the temperature was found to be uniform along the height of the two-phase region. However, during transients it is expected that this temperature may vary as a function of time and space as the decay heat rate and void distribution change with time. The dominant mode of heat transfer in this region was found by these authors to be convection. Convection took place as a result of vertical counter-current flow of vapor and liquid. Bau and Torrance [6] also concluded from their temperature measurements in a single-phase region above a two-phase region, that the dominant mode of heat transfer was by conduction; because of higher heat transfer rates from the top of bed, the maximum temperature occurs in the lower part of the bed. Therefore, we expect single-phase regions to prevail above and below the two-phase region at least until the two-phase region propagates to the rest of the bed. In concurrence with the findings of Bau and Torrance, conduction will be assumed to be the dominant mode of heat transfer in

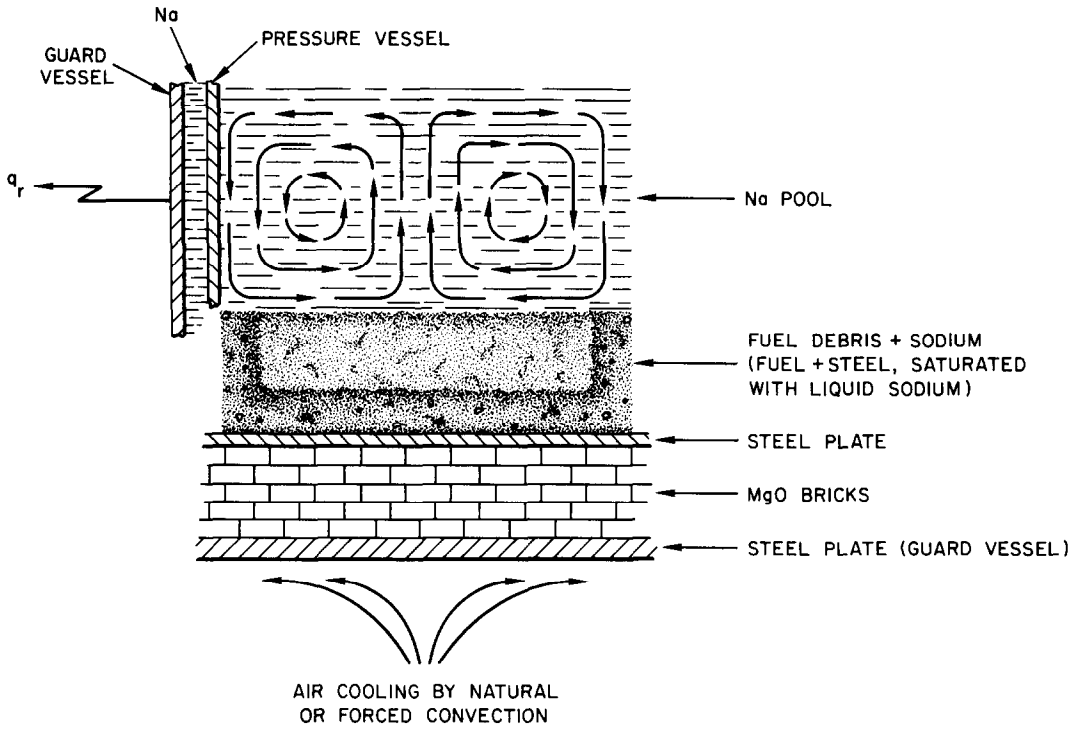

FIG. 1. Schematic of design features for in-vessel core debris retention.

these single-phase regions. In the sodium above the bed, natural convection will be assumed to be the dominant mode of heat transfer. Three regions, namely a liquid zone at the bottom designated region 1, a two-phase region in the middle designated region 2, and a top liquid region designated region 3, are described by the governing equations derived in the following sections.

GOVERNING EQUATIONS FOR SINGLE-PHASE REGIONS

As discussed previously, heat transfer in these two regions is conduction dominated, described by the following governing equations. Assuming the bed to consist of fuel and steel particles, then for sodium-saturated regions, we have for a porous bed with constant properties

$$\rho C_p \frac{\partial T_i}{\partial t} = K \frac{\partial^2 T_i}{\partial y^2} + \dot{Q}, \quad i = 1 \text{ or } 3 \tag{1a}$$

where the volumetric heat capacity, ρC_p, of the liquid-saturated bed is given by

$$\rho C_p = \varepsilon_F \rho_F C_{PF} + \varepsilon_s \rho_s C_{ps} + \varepsilon \rho_{Na} C_{pNa} \tag{1b}$$

and the thermal conductivity, K, as [11]

$$K = K_{Na}\left[1 - \frac{(1-\varepsilon)(K_{Na}/K_{FS}-1)}{1+(1-\varepsilon)^{1/3}(K_{Na}/K_{SE}-1)}\right] \tag{1c}$$

with K_{SE} given by the Maxwell relation

$$K_{SE} = K_1 \frac{3-3\alpha_v+2\alpha_v K_1/K_2}{(3-\alpha_v)K_1/K_2+\alpha_v} \tag{1d}$$

where $\alpha_v = \varepsilon_1/(1-\varepsilon)$. Subscript 1 refers to the solids with the largest volume fraction and 2 refers to the solids with the smallest volume fraction. The values predicted by this expression appear to agree with measured values [12] of thermal conductivity of sodium-saturated fuel debris. The symbols ε_F, ε_s, and ε denote, respectively, the volume fractions (of the total volume of bed) of fuel, stainless steel and void. It is convenient to express ε_F, ε_s, and ε in terms of bed loadings of these materials. Thus,

$$\varepsilon_F = \frac{(1-\varepsilon)(B_F/\rho_F)}{B_F/\rho_F + B_s/\rho_s}, \quad \varepsilon_s = \frac{(1-\varepsilon)B_s/\rho_s}{B_F/\rho_F + B_s/\rho_s} \tag{2a}$$

$$\varepsilon = 0.593 - 1.23 \times 10^{-4} B \tag{2b}$$

where $B = B_F + B_s$, the total bed loading in kg m^{-2}.

The above expression for ε was obtained empirically by Gabor *et al.* [1]. The internal heat generation $\dot{Q}$ is expressed per unit volume of the bed and is related to microscopic decay rate $\dot{q}$ per unit volume of the fuel

$$\dot{Q} = \varepsilon_F \dot{q}. \tag{3}$$

GOVERNING EQUATIONS FOR TWO-PHASE REGION

The analysis of void propagation, heat transfer and hydrodynamics in the two-phase region can be carried

out through the methodology of two-phase flows in porous media. The superficial velocities of liquid denoted by u_f, and of vapor, denoted by u_g, can be expressed by Darcy's law for two-phase flows:

$$u_f = -\frac{kk_{rf}}{\mu_f}\left(\frac{\partial P_f}{\partial x} + \rho_f g\right) \quad (4)$$

$$u_g = -\frac{kk_{rg}}{\mu_g}\left(\frac{\partial P_g}{\partial x} + \rho_g g\right). \quad (5)$$

These superficial velocities are related to interstitial velocities v_f and v_g through

$$u_f = \varepsilon s v_f, \quad u_g = \varepsilon(1-s)v_g \quad (6)$$

where s is the saturation, defined as the fraction of void volume occupied by liquid phase. Here, k_{rf} and k_{rg} are the relative permeabilities of the liquid and vapor phases, respectively. Each varies from a value of 0 (if the phase is immobile) to 1 (if only that phase exists). Consequently, these relative permeabilities account for the decrease in the mobility of one phase due to the presence of the second.

The difference between vapor pressure and liquid pressure is the capillary pressure P_c given as

$$P_c = P_g - P_f. \quad (7)$$

From equations of conservation of mass we have for the liquid phase:

$$\varepsilon\frac{\partial \rho_f s}{\partial t} + \frac{\partial}{\partial y}(\rho_f u_f) = -\Gamma \quad (8a)$$

and for the vapor phase

$$\varepsilon\frac{\partial \rho_g(1-s)}{\partial t} + \frac{\partial}{\partial y}(\rho_g u_g) = \Gamma \quad (8b)$$

where Γ is the rate of generation of vapor per unit volume. The sum of these two equations yields the equation for the mixture as

$$\varepsilon\frac{\partial}{\partial t}[s\rho_f + (1-s)\rho_g] + \frac{\partial}{\partial y}(\rho_f u_f + \rho_g u_g) = 0. \quad (9)$$

Assuming the liquid coolant is superheated at the pressure in the vapor phase, and the liquid phase and solid phase are at the same temperature, the energy equation for the solid phase can be written as

$$(\varepsilon_F \rho_F C_{pF} + \varepsilon_s \rho_s C_{ps})\frac{\partial T}{\partial t} = K_{FS}\frac{\partial^2 T}{\partial y^2} - q_w \frac{A_S}{V} + \dot{Q} \quad (10)$$

where A_S in total surface area of the solid particles and $K_{FS} = (1-\varepsilon)K_{SE}$. For a two-phase mixture, the energy equation is given as

$$\frac{\partial}{\partial t}[\varepsilon s\rho_f h_f + \varepsilon(1-s)\rho_g h_g] + \frac{\partial}{\partial y}(\rho_f u_f h_f + \rho_g u_g h_g) = \frac{q_w A_S}{V} + \frac{\partial}{\partial y}\left(K_{2\Phi}\frac{\partial T}{\partial y}\right) \quad (11a)$$

where $K_{2\Phi}$ is the thermal conductivity of the two-phase mixture. Upon neglecting vapor-phase conductivity, $K_{2\Phi}$ can be given as

$$K_{2\Phi} \simeq \varepsilon s K_f. \quad (11b)$$

The use of equation (9) in equation (11a) gives,

$$\rho_f C_{pf}\left(\varepsilon s\frac{\partial T}{\partial t} + u_f\frac{\partial T}{\partial y}\right) + \varepsilon(1-s)\rho_g\frac{\partial h_g}{\partial t} + \rho_g u_g\frac{\partial h_g}{\partial y} + \Gamma\Delta h = \frac{q_w A_S}{V} + \frac{\partial}{\partial y}\left(K_{2\Phi}\frac{\partial T}{\partial y}\right) \quad (11c)$$

where $\Delta h = h_g - h_f$. Assuming $h_g \simeq h_g(P_g)$, equation (11c) gives

$$\Gamma = \frac{1}{\Delta h}\left[\frac{q_w A_S}{V} + \frac{\partial}{\partial y}\left(K_{2\Phi}\frac{\partial T}{\partial y}\right) - \varepsilon(1-s)\rho_g\frac{\partial h_g}{\partial P_g}\frac{\partial P_g}{\partial t} - \rho_g u_g\frac{\partial h_g}{\partial P_g}\frac{\partial P_g}{\partial y} - \rho_f C_{pf}\left(\varepsilon s\frac{\partial T}{\partial t} + u_f\frac{\partial T}{\partial y}\right)\right]. \quad (12a)$$

If, as assumed, the vapor pressure gradient is small and is changing slowly with time, the above equation becomes

$$\Gamma \simeq \frac{1}{\Delta h}\left[\frac{q_w A_S}{V} + \frac{\partial}{\partial y}\left(K_{2\Phi}\frac{\partial T}{\partial y}\right) - \rho_f C_{pf}\left(\varepsilon s\frac{\partial T}{\partial t} + u_f\frac{\partial T}{\partial y}\right)\right]. \quad (12b)$$

VOID PROPAGATION EQUATION

Assuming two-phase flow to be incompressible, equations (8) and (9) simplify to

$$\varepsilon\frac{\partial s}{\partial t} + \frac{\partial u_f}{\partial y} = -\frac{\Gamma}{\rho_f} \quad (13)$$

$$-\varepsilon\frac{\partial s}{\partial t} + \frac{\partial u_g}{\partial y} = \frac{\Gamma}{\rho_g}. \quad (14)$$

The combination of these equations yields

$$\frac{\partial(u_f + u_g)}{\partial y} = \Gamma\left(\frac{1}{\rho_g} - \frac{1}{\rho_f}\right) \simeq \frac{\Gamma}{\rho_g} \quad (15)$$

$$u_f + u_g = \int_{Y_1}^{y}\frac{\Gamma}{\rho_g}\,dy, \quad (16)$$

where Y_1 is the position of the lower interface between two-phase and single-phase regions.

The combination of equations (4), (5) and (7) gives

$$\frac{\partial(P_g - P_f)}{\partial y} = \frac{\partial P_c}{\partial y} = \frac{u_f\mu_f}{kk_{rf}} - \frac{u_g\mu_g}{kk_{rg}} + (\rho_f - \rho_g)g. \quad (17)$$

Eliminating u_g between equations (5) and (17), we

obtain

$$u_f = \frac{\mu_g/k_{rg}}{\mu_g/k_{rg}+\mu_f/k_{rf}}\int_{Y_1}^{y}\frac{\Gamma}{\rho_g}\,dy - \frac{k(\rho_f-\rho_g)g}{(\mu_g/k_{rg}+\mu_f/k_{rf})} + \frac{k}{\mu_g/k_{rg}+\mu_f/k_{rf}}\frac{\partial P_c}{\partial s}\frac{\partial s}{\partial y}, \quad (18a)$$

where it is assumed that capillary pressure is a function of saturation only. The substitution of equation (18a) in equation (5) yields

$$u_g = \frac{\mu_f/k_{rf}}{\mu_f/k_{rf}+\mu_g/k_{rg}}\int_{Y_1}^{y}\frac{\Gamma}{\rho_g}\,dy + \frac{k(\rho_f-\rho_g)g}{\mu_f/k_{rf}+\mu_g/k_{rg}} - \frac{k}{\mu_f/k_{rf}+\mu_g/k_{rg}}\frac{\partial P_c}{\partial s}\frac{\partial s}{\partial y}. \quad (18b)$$

Assuming relative permeabilities to be a function of saturation only (see Appendix A), we obtain from the above equation

$$\frac{\partial u_g}{\partial y} = \frac{\partial F}{\partial s}\frac{\partial s}{\partial y} + \left(\int_{Y_1}^{y}\frac{\Gamma}{\rho_g}\,dy\right)\frac{\partial \Psi}{\partial s}\frac{\partial s}{\partial y} + \Psi\frac{\Gamma}{\rho_g} - \frac{\partial}{\partial y}\left(\Phi\frac{\partial s}{\partial y}\right), \quad (19)$$

where

$$F = \frac{k(\rho_f-\rho_g)g}{\mu_f/k_{rf}+\mu_g/k_{rg}}, \quad \Psi = \frac{\mu_f/k_{rf}}{\mu_f/k_{rf}+\mu_g/k_{rg}}, \quad (20a)$$

$$\Phi = -\frac{k}{\mu_f/k_{rf}+\mu_g/k_{rg}}\frac{\partial P_c}{\partial(1-s)}. \quad (20b)$$

Substituting equation (19) in equation (14) gives

$$\frac{\partial \alpha}{\partial t} + V_\alpha\frac{\partial \alpha}{\partial y} = \frac{\partial}{\partial y}\left(D_\alpha\frac{\partial \alpha}{\partial y}\right)+\Omega, \quad (21a)$$

where

$$\alpha = 1-s, \quad V_\alpha = \frac{1}{\varepsilon}\left[\frac{\partial F}{\partial \alpha}+\left(\int_{Y_1}^{y}\frac{\Gamma}{\rho_g}\,dy\right)\frac{\partial \Psi}{\partial \alpha}\right], \quad (21b)$$

$$D_\alpha = \frac{\Phi}{\varepsilon}\Omega = (1-\Psi)\frac{\Gamma}{\varepsilon\rho_g}. \quad (21c)$$

CONCLUDING REMARKS

Equation (21a) gives the transient and spatial response of volumetric concentration, α, of vapor phase in a porous body. There have been a number of other derivations of this equation; however, none of these have considered the phase change (see, for example, refs. [13–15]). The above equation is analogous to the void propagation equation originally developed by Zuber and Staub [16] for two-phase flows in pipes and channels. In their terminology, V_α is referred to as the velocity of propagation of volumetric concentration wave, Ω as the reaction frequency, and D_α as the diffusion coefficient. However, the individual terms making up these parameters for porous media flows appear somewhat different from those for nonporous media. This distinction arises owing to the fact that the flows through the porous media are formulated in terms of Darcy's law, whereas nonporous media flows are traditionally formulated in terms of drift velocity.

To determine void propagation, equation (21a) is solved in conjunction with equations (10) and (12). The relevant boundary conditions are derived in Appendix B.

REFERENCES

1. J. D. Gabor, E. S. Sowa, L. Baker, Jr and J. C. Cassulo, Studies and experiments on heat removal from fuel debris in sodium, CONF-740401-P2, *Proc. ANS Fast Reactor Safety Meeting*, Beverly Hills, p. 823 (1974).
2. R. J. Lipinski, A model for boiling and dryout in particle beds, SAND82-0765 (NUREG/CR-2646), Sandia National Laboratories (June 1982).
3. B. D. Turland and K. Moore, One-dimensional models of boiling and dry-out. In *Proc Fifth Post Accident Heat Removal Information Exchange Meeting*, Nuclear Research Center, Karlsruhe, F.R.G. (1983).
4. V. K. Dhir and I. Catton, Prediction of dryout heat fluxes in bed of volumetrically heated particles, *Proc. Int. Meeting on Fast Reactor Safety and Related Physics*, Chicago, CONF-761001, p. 2026 (1976).
5. E. B. Bergeron, A. One-dimensional time-dependent debris bed model, *Proc. ASME/JSME Thermal Engineering Joint Conference*, Vol. 2, p. 23 (1983).
6. H. H. Bau, and K. E. Torrance, Boiling in low-permeability porous materials, *Int. J. Heat Mass Transfer* **25**, 45 (1982).
7. K. S. Udell, Heat transfer in porous media heated from above with evaporation, condensation, and capillary effects, *Trans. Am. Soc. mech. Engrs*, Series C, *J. Heat Transfer* **105**, 485 (1983).
8. C. H. Sondergeld and D. L. Turcotte, An experimental study of two-phase convection in a porous medium with applications to geological problems, *J. geophys. Res.* **82**, 2045 (1977).
9. C. H. Sondergeld and D. L. Turcotte, Flow visualization studies of two-phase thermal convection in a porous layer, *Pure Appl. Geophys.* **117**, 321 (1978).
10. D. O. Lee and R. H. Nilson, Flow visualization in heat-generating porous media, Sandia National Laboratories, Albuquerque, SAND76-0614 (1977).
11. H. Kampf and G. Karsten, Effects of different types of void volumes on the radial temperature distribution of fuel pins, *Nucl. Applic. Technol.* **9**, 288 (1970).
12. E. Gronager, M. Schwarz and R. J. Lipinski, PAHR Debris Bed Experiment D-4, Sandia National Laboratories, Albuquerque, SAND80-2146 (1981).
13. C. M. Marle, *Multiphase Flow in Porous Media*. Gulf, Houston (1981).
14. R. A. Greenkarn, *Flow Phenomena in Porous Media*. Marcel Dekker, New York (1983).
15. J. Bear, *Dynamics of Fluids in Porous Media*. American Elsevier, New York (1972).
16. N. Zuber, and F. N. Staub, The propagation and the wave form of the vapor volumetric concentration in boiling, forced convection system under oscillatory condition, *Int. J. Heat Mass Transfer* **9**, 871 (1966).

APPENDIX A: CONSTITUTIVE RELATIONSHIPS

Relative permeabilities

The relative permeabilities k_{rf} and k_{rg} of the porous media introduced in Darcy law for two-phase flow [see equations (2) and (3)], are expressed as the fractions of the total permeability k. Experiments indicate that these coefficients are primarily a function of saturation but they are difficult to obtain experimentally. For the sake of simplicity and for the lack of any better information, we will choose the following linear forms

$$k_{rf} = s, \quad k_{rg} = 1-s. \tag{A1}$$

Thus, in the above choice the respective relative permeabilities represent the ratio of cross sections available for liquid and vapor flows, and have values between 0 and 1. These forms have been suggested by Bau and Torrance [6]. These forms are consistent with the physics of two-phase flow in channels.

Permeability

The permeability k is obtained from the well-known empirical correlation by Kozeny-Carman [15]

$$k = \frac{D^2}{150}\frac{\varepsilon^3}{(1-\varepsilon)^2} \tag{A2}$$

where D is the average particle diameter.

Heat flux from solid particulate

The majority of constitutive relationships are obtained from steady-state experiments and analyses. For the lack of any better information we will pursue this course for obtaining heat flux q_w [see equation (11)]. For simplicity, it will be assumed that axial conduction in the two-phase flow region is negligible, implying nearly constant temperature in the axial direction. There are ample experimental data (see, for example, refs. [6] and [7]) available that support this assumption. Furthermore, it will be assumed that vapor and liquid are in thermal equilibrium and that

$$P_f = P_g = P. \tag{A3}$$

In view of the above assumptions, equations (6)–(8), (10), (11) and (17) become, respectively,

$$\frac{\partial}{\partial y}(\rho_f u_f) = -\Gamma \tag{A4}$$

$$\frac{\partial}{\partial y}(\rho_g u_g) = \Gamma \tag{A5}$$

$$\frac{\partial}{\partial y}(\rho_f u_f + \rho_g u_g) = 0 \tag{A6}$$

$$h_f \frac{\partial}{\partial y}(\rho_f u_f) + h_g \frac{\partial}{\partial y}(\rho_g u_g) = \frac{q_w A_S}{V} \tag{A7}$$

$$\frac{\rho_f u_f v_f}{ks} - \frac{\rho_g u_g v_g}{k(1-s)} + \Delta\rho g = 0 \tag{A8}$$

where in the last equation we have used equation (A1). The use of equations (A4) and (A5) in equation (A7) gives

$$\Gamma = \frac{q_w A_S}{V\Delta h}. \tag{A9}$$

For spherical particles A_S/V is given as

$$\frac{A_S}{V} = \frac{N\pi D^2}{N\pi D^3/6(1-\varepsilon)} = \frac{6(1-\varepsilon)}{D}. \tag{A10}$$

The use of equation (A10) in equation (A9) gives

$$\Gamma = \frac{6q_w(1-\varepsilon)}{D\Delta h}. \tag{A11}$$

The integration of equation (A6) gives

$$\rho_f u_f = -\rho_g u_g = -\dot{m}_v \tag{A12}$$

where we have implicitly used the fact that during steady state the interfaces are stationary, that is, $\dot{Y}_1 = \dot{Y}_2 = 0$, so that there is no net flow across either interface [see equations (B5) and (B6)].

The substitution of equation (A10) in equation (A8) gives

$$\dot{m}_v = \frac{s(1-s)k\Delta\rho g}{(1-s)v_f + sv_g}. \tag{A13}$$

The integration of equation (A4) gives

$$\rho_f u_f = -\int_{Y_1}^{y} \Gamma \, dy. \tag{A14}$$

The substitution of equation (A11) in equation (A14) yields

$$\dot{m}_v = \frac{q_w A_S (y-Y_1)}{V\Delta h} = \frac{6q_w(1-\varepsilon)}{D\Delta h}(y-Y_1). \tag{A15}$$

The substitution of equation (A15) into equation (A13) gives

$$\frac{q_w A_S}{V} = \frac{[s(1-s)k\Delta\rho g]\Delta h}{[(1-s)v_f + sv_g](y-Y_1)}. \tag{A16}$$

The above equation provides heat flux q_w for use in equations (9) and (12).

APPENDIX B: INTERFACE BALANCE EQUATIONS

To describe the motion of the interface between single-phase and two-phase regions, we need to obtain interface balances of mass and energy. For this purpose the interface is assumed to be smooth and sharply defined. Consider a thin elementary strip across the interface, as shown in Fig. B1. Let coordinates of an interface be denoted by $Y_i(t)$ and of the strip as $Y_{iL}(t)$ and $Y_{iU}(t)$ (see Fig. B1). These interface balances are obtained by integrating the following general equation of mass and energy across the interface over the strip.

Mass:

$$\varepsilon\frac{\partial}{\partial t}[s\rho_f + (1-s)\rho_g] + \frac{\partial}{\partial y}(\rho_f u_f + \rho_g u_g) = 0. \tag{B1}$$

Energy:

$$\frac{\partial}{\partial t}[\varepsilon_F\rho_F C_{PF}T + \varepsilon_s\rho_s C_{ps}T + \varepsilon s\rho_f h_f + \varepsilon(1-s)\rho_g h_g] + \frac{\partial}{\partial y}[\rho_f u_f h_f + \rho_g u_g h_g] = \frac{\partial}{\partial y}\left(K\frac{\partial T}{\partial y}\right) + \dot{Q}. \tag{B2}$$

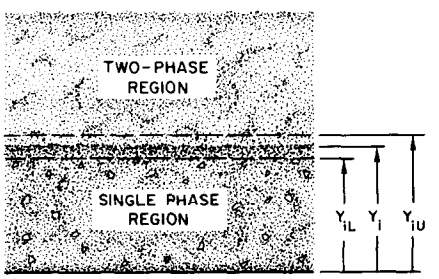

FIG. B1. Control volume for interface balances between two-phase and single-phase regions during sodium boiling.

Integrating equation (B1) gives

$$\varepsilon\int_{Y_{iL}}^{Y_{iU}}\frac{\partial}{\partial t}[s\rho_f+(1-s)\rho_g]\,dy + \int_{Y_{iL}}^{Y_{iu}}\frac{\partial}{\partial y}(\rho_f u_f+\rho_g u_g)\,dy=0. \quad (B3)$$

The application of Leibnitz' rule gives

$$\varepsilon\frac{\partial}{\partial t}\int_{Y_{iL}}^{Y_{iU}}[s\rho_f+(1-s)\rho_g]\,dy-\varepsilon[s\rho_f+(1-s)\rho_g]|_{Y_{iU}}\times\frac{dY_{iU}}{dt}+\varepsilon[s\rho_f+(1-s)\rho_g]|_{Y_{iL}}\frac{dY_{iL}}{dt}+(\rho_f u_f+\rho_g u_g)|_{Y_{iU}}-(\rho_f u_f+\rho_g u_g)|_{Y_{iL}}=0. \quad (B4)$$

Taking the limit of Y_{iL} and Y_{iU} approaching Y_i, we obtain for the interface between single-phase region 1 and two-phase region 2,

$$-\varepsilon[s\rho_f+(1-s)\rho_g]|_{Y_i^+}\dot{Y}_1+\varepsilon\rho_f\dot{Y}_1+(\rho_f u_f+\rho_g u_g)|_{Y_i^+}=0. \quad (B5)$$

Similarly, for the interface between two-phase region 2 and single-phase region 3

$$-\varepsilon\rho_f\dot{Y}_2+\varepsilon[s\rho_f+(1-s)\rho_g]|_{Y_2^-}\dot{Y}_2-(\rho_f u_f+\rho_g u_g)|_{Y_2^-}=0. \quad (B6)$$

Similarly, the integration of the energy equation across an interface yields

$$\frac{\partial}{\partial t}\int_{Y_{iL}}^{Y_{iU}}[\varepsilon_F\rho_F C_{PF}T+\varepsilon_s\rho_s C_{ps}T+\varepsilon s\rho_f h_f+\varepsilon(1-s)\rho_g h_g]\,dy -[\varepsilon_F\rho_F C_{PF}T+\varepsilon_s\rho_s C_{ps}T+\varepsilon s\rho_f h_f+\varepsilon(1-s)\rho_g h_g]|_{Y_{iU}}\dot{Y}_{iU} +[\varepsilon_F\rho_F C_{PF}T+\varepsilon_s\rho_s C_{ps}T+\varepsilon s\rho_f h_f+\varepsilon(1-s)\rho_g h_g]|_{Y_{iL}}\dot{Y}_{iL} +[\rho_f u_f h_f+\rho_g u_g h_g]|_{Y_{iU}}-[\rho_f u_f h_f+\rho_g u_g h_g]_{Y_{iL}} = K\frac{\partial T}{\partial y}\bigg|_{Y_{iU}}-K\frac{\partial T}{\partial y}\bigg|_{Y_{iL}}+\int_{Y_{iL}}^{Y_{iU}}\dot{Q}\,dy. \quad (B7)$$

Taking the limit of Y_{iL} and Y_{iu} approaching Y_i and assuming the temperature is continuous across the interface, we obtain for the interface between single-phase region 1 and two-phase region 2

$$-[\varepsilon s\rho_f h_f+\varepsilon(1-s)\rho_g h_g]|_{Y_i^+}\dot{Y}_1+\varepsilon\rho_f h_f|_{Y_i^-}\dot{Y}_1 +(\rho_f u_f h_f+\rho_g u_g h_g)|_{Y_i^+} = K\frac{\partial T}{\partial y}\bigg|_{Y_i^+}-K\frac{\partial T}{\partial y}\bigg|_{Y_i^-}. \quad (B8)$$

For the interface between two-phase region 2 and single-phase region 3, we obtain

$$-\varepsilon\rho_f h_f\dot{Y}_2+[\varepsilon s\rho_f h_f+\varepsilon(1-s)\rho_g h_g]|_{Y_2^-}\dot{Y}_2-(\rho_f u_f h_f+\rho_g u_g h_g)|_{Y_2^-} = K\frac{\partial T}{\partial y}\bigg|_{Y_2^+}-K\frac{\partial T}{\partial y}\bigg|_{Y_2^-}. \quad (B9)$$

Boundary conditions at interfaces

To solve the transient void propagation equation (21), boundary conditions at the interfaces between the single-phase regions and the two-phase region need to be prescribed.

Top interface. The top part of the two-phase region is subcooled and, consequently, vapor rising from the lower parts condenses in this part and the top interface defines the end point up to which vapor can penetrate. Consequently, it can logically be assumed that at the top interface,

$$u_g|_{Y_2}=0. \quad (B10)$$

The use of equation (B10) in equation (B6) yields

$$\rho_f u_f=-\varepsilon(1-s)\Delta\rho\dot{Y}_2 \quad (B11)$$

where $\Delta\rho=\rho_f-\rho_g$. The substitution of equation (B11) in equation (B9) gives

$$\varepsilon(1-s)\rho_g\Delta h\dot{Y}_2=K\frac{\partial T}{\partial y}\bigg|_{Y_2^+}-K\frac{\partial T}{\partial y}\bigg|_{Y_2^-}. \quad (B12)$$

If we further assume that at the upper interface $P_g=P_f$, then

$$P_c|_{Y_2}=0. \quad (B13)$$

The use of equations (B10), (B11) and (B13) in equation (17) gives

$$\frac{k_{rf}(s)}{1-s}=\frac{\varepsilon\nu_f}{kg}\dot{Y}_2. \quad (B14)$$

Since k_{rf} is a function of saturation only [see equation (A1)], equation (B14) provides the boundary condition for s at the top boundary for solution of void propagation equation (21).

Bottom interface. Since the bottom of the debris bed is closed, the region below the interface is expected to behave like a large liquid pool in to which liquid film from the two-phase region will drain. Consequently, the liquid surface at the interface can be approximately thought of as a stagnation surface for the liquid draining at the interface from the two-phase region. This, in turn, implies that the following condition can be assumed

$$u_f|_{Y_i}=0. \quad (B15)$$

The use of the above condition in equation (B5) gives

$$\rho_g u_g|_{Y_i^+}=-\varepsilon(1-s)\Delta\rho\dot{Y}_1. \quad (B16)$$

The substitution of equations (B15) and (B16) in equation (B8) gives

$$\varepsilon(1-s)\rho_f\Delta h\dot{Y}_1=K\frac{\partial T}{\partial y}\bigg|_{Y_i^+}-K\frac{\partial T}{\partial y}\bigg|_{Y_i^-}. \quad (B17)$$

The use of equations (B15) and (B16) in equation (17) gives

$$\frac{\partial P_c}{\partial s}\frac{\partial s}{\partial y}\bigg|_{Y_i^+}=\frac{\varepsilon(1-s)\Delta\rho\nu_g}{kk_{rg}}\dot{Y}_1+\Delta\rho g \quad (B18)$$

which provides the boundary condition for s for equation (21) at the lower interface.

EQUATIONS DU TRANSFERT DE CHALEUR ET DE MASSE DANS LES LITS POREUX GENERANT DE LA CHALEUR—I. EBULLITION DE REFROIDISSEMENT ET PROPAGATION VARIABLE DU VIDE

Résumé—Une proposition est faite de revêtir la base du récipient de garde avec des briques de magnésie (MgO) pour retenir le noyau de débris qui suit un accident de rupture. Avec la conduction comme mode dominant de transfert thermique dans le lit de débris et la convection naturelle dans le liquide environment, le lit de débris complètement submergé dans le sodium réfrigérant peut réaliser une ébullition de refroidissement. Une équation est écrite pour déterminer la distribution variable du vide pendant l'ébullition. Les aspects variables de cette distribution sont trouvés être importants pour des lits très profonds et pendant la trempe du lit. Le terme de source de production de vapeur est obtenue à partir de la solution de l'équation d'énergie pour le réfrigérant diphasique, tandis que la distribution de température dans la phase solide est calculée à partir de l'équation de conduction. Le flux thermique à partir des particules de combustible dans le réfrigérant diphasique est modélisé à partir de la solution des équations de continuité diphasique, de la quantité de mouvement et de l'énergie.

GLEICHUNGEN FÜR DEN WÄRME- UND STOFFÜBERGANG IN WÄRMEFREISETZENDEN PORÖSEN SCHÜTTUNGEN—I. SIEDEN DES KÜHLMITTELS UND INSTATIONÄRE DAMPFAUSBREITUNG

Zusammenfassung—Es ist als Konstruktions-Variante vorgeschlagen worden, den Boden des Sicherheitsbehälters mit Magnesia (Mg0) auszukleiden. Nach einem Unfall, bei dem das Core zerstört worden ist, sollen so die Trümmer zurückgehalten werden. In der Trümmer-Schüttung ist Wärmeleitung die bestimmende Art der Wärmeübertragung, im darüber befindlichen Behälter ist es natürliche Konvektion. Die Trümmer-Schüttung, die vollständig von dem Kühlmittel Natrium überflutet ist, kann anfangen sich aufzuwärmen, wobei schließlich das Kühlmittel zu sieden beginnt. Zur Berechnung der instationären Dampfausbreitung während des Siedens wird einen Gleichung entwickelt. Die instationären Aspekte der Dampfausbreitung werden bei tiefen Schüttungen und während der Abschreckphase für besonders wichtig gehalten. Der Dampferzeugungs-Term ergibt sich aus der Lösung der Energiegleichung für das zweiphasige Kühlmittel, die Temperaturverteilung in der festen Phase aus der Wärmeleitgleichung. Die Wärmestromdichte im Brennstoff wird durch Lösen der stationären zweiphasigen Kontinuitäts-, Impuls- und Energiegleichungen berechnet.

УРАВНЕНИЯ ТЕПЛО- И МАССОПЕРЕНОСА В ТЕПЛОВЫДЕЛЯЮЩИХ ПОРИСТЫХ СЛОЯХ—I. КИНЕТИКА ОХЛАЖДЕНИЯ И ЭВОЛЮЦИЯ ПУЗЫРЬКА

Аннотация—Как одно из важных конструктивных решений предложена футеровка кирпичами из окиси магния дна защитной оболочки ядерного реактора с целью предотвращения выброса радиоактивных осколков при его аварии. Из-за теплопроводности, являющейся доминирующим механизмом теплопереноса в тепловыделяющем слое, и естественной конвекции в объеме над его поверхностью, слой, будучи помещенным в натриевый охладитель, может вызвать нагрев и кипение последнего. Получено уравнение, которое описывает движение и эволюцию пузырька во время кипения. Предполагается, что характер движения пузырьков и их эволюция являются существенными для очень глубоких слоев во время их резкого охлаждения. Слагаемое в уравнении, отвечающее за скорость парообразования, получено из решения уравнения энергии для двухфазного охладителя, тогда как поле температуры в твердой фазе получено из решения уравнения теплопроводности. Тепловой поток от частицы топлива к двухфазному охладителю моделируется на основании решения стационарных уравнений неразрывности, импульса и энергии для двухфазной среды.